ELSEVIER

J. Non-Newtonian Fluid Mech. xxx (2007) xxx–xxx

Journal of Non-Newtonian Fluid Mechanics

www.elsevier.com/locate/jnnfm

Interfacial instability between sheared elastic liquids in a channel

J.C. Miller [a,b,*,1], J.M. Rallison [a]

[a] *Department of Applied Mathematics and Theoretical Physics, University of Cambridge, Cambridge CB3 0WA, UK*
[b] *Mathematical Modeling & Analysis Group and Center for Nonlinear Studies, MS B284, Los Alamos National Laboratory, Los Alamos, NM 87545, USA*

Received 6 July 2006; received in revised form 11 January 2007; accepted 24 January 2007

Abstract

We consider the linear stability of the interface between two sheared elastic liquids at large Weissenberg number (*Wi*) with negligible inertia. The liquids are of Oldroyd-B or UCM type and have matched viscosity. In UCM liquids, Renardy [Y. Renardy, Stability of the interface in two-layer Couette flow of upper convected Maxwell liquids, J. Non-Newton. Fluid Mech. 28 (1988) 99–115] found a purely elastic instability for short-waves in the absence of surface tension for which the perturbation flow decays exponentially away from the interface. For UCM liquids at large *Wi* we show that this instability persists even though the wavelength is larger than the channel width and the disturbance occupies the entire channel. Surprisingly, the growth rate is not affected by the location of the walls, even though the mode structure is altered. This analysis suggests a reappraisal of the appropriateness of the *short-wave* and *long-wave* classifications for instabilities of viscoelastic liquids in order to accommodate the additional length scale introduced by fluid velocity and relaxation. The instability persists for Oldroyd-B liquids even as the elastic contribution to viscosity approaches zero. Surprisingly too, the inclusion of surface tension does not affect the asymptotic growth rate at large wavenumber. When more modest values of *Wi* are considered, we find parameter values for which arbitrarily large surface tension reduces the growth rate but does not stabilize the flow; previously proposed mechanisms based on the interface displacement are therefore inadequate to explain the instability. Because the instability is locally generated, it appears in other high *Wi* flows with interfaces, both in channels and in pipes.
© 2007 Elsevier B.V. All rights reserved.

Keywords: Elastic instability; Interfacial instability; Channel flow; Surface tension

1. Introduction

Viscoelastic flows are important in a number of industrial applications and their instabilities have received considerable attention. The elasticity provides a source of energy for instabilities even in the absence of inertia, creating a class of *purely elastic* instabilities. Reviews of purely elastic instabilities can be found in [2,3]. In this paper, we study the stability to disturbances with wavenumber k of two inertialess Upper Convected Maxwell (UCM) or Oldroyd-B liquids. The liquids undergo shear in a channel of width L with characteristic velocity U_0; their viscosities are matched, but their relaxation times differ.

Much of the theoretical investigation of inertialess interfacial instabilities in viscoelastic liquids began with Chen [4] in the long-wave (wavelength long compared to channel width: $L \ll k^{-1}$) limit and with Chen & Joseph and Renardy [1,5] in the short-wave (wavelength short compared to channel width: $k^{-1} \ll L$) limit. The physical mechanism behind the long-wave instability was provided by Hinch et al. [6]. Related theoretical work in both limits was done by Ganpule and Khomami [7–9]. The results were generalized for other liquids by Wilson [10] and Wilson and Rallison [11–13].

Inertialess Couette flow of two Newtonian liquids with matched viscosity is linearly stable, as is the inertialess Couette flow of a single Oldroyd-B liquid [14,15]. A nonlinear stability proof for UCM liquids in Poiseuille flow is claimed by [16] who showed that the flow minimized an energy functional, but recent work [17,18] shows that no reasonable energy functional will decay monotonically in time for Oldroyd-B or UCM liquids. This is further confirmed by some numerical simulations [19] which find a finite amplitude nonlinear instability of Poiseuille and Couette channel flow for Oldroyd-B liquids when the elastic component of viscosity is large compared to the Newtonian component of viscosity.

Because the Couette flow of a single inertialess Oldroyd-B liquid is linearly stable, the short and long-wave interfacial instabilities must be attributed to the jump in elastic properties at the

* Corresponding author.
E-mail address: jomiller@lanl.gov (J.C. Miller).
[1] Los Alamos Report LA-UR-06-0420.

0377-0257/$ – see front matter © 2007 Elsevier B.V. All rights reserved.
doi:10.1016/j.jnnfm.2007.01.009

Please cite this article in press as: J.C. Miller, J.M. Rallison, Interfacial instability between sheared elastic liquids in a channel, J. Non-Newtonian Fluid Mech. (2007), doi:10.1016/j.jnnfm.2007.01.009

interface. The wavespeed of the long-wave mode relative to the interface is found to be much less than the velocity scale defined by the wavelength and the growth rate, that is, at leading order the wave remains stationary relative to the interface. This reflects the fact that the instability can be explained in terms of the normal stress jump which is independent of the sign of the shear rate [6]. In contrast, the short-wave mode travels with a relative speed comparable to the velocity scale defined by its growth rate and wavelength. The physical mechanism must involve some effect which depends on the sign of the shear rate. Some mechanisms have been suggested for this instability that depend on interface displacement [9,20]. We show, however, that at sufficiently large Weissenberg number this instability exists even if the interface is held flat by surface tension, so a different explanation is needed.

Renardy [1] considered interfacial instabilities of inertialess Couette flow of UCM liquids for short-waves: $k^{-1} \ll L$. She found that the perturbed flow is localized in a boundary layer of thickness $1/k$ near the interface. Consequently short-wave instabilities exist provided the walls are sufficiently far from the interface. In the large Weissenberg number limit, she found that the growth rate is a function only of the ratio of the two relaxation times. For some ratios the flow is stable. In contrast, at low Weissenberg number, all pairs of relaxation times are unstable. The two limits involve different mechanisms. This paper focuses on the large Weissenberg number limit.

Chen and Joseph [5] examined inertialess core-annular flow of UCM liquids through a pipe without surface tension. They found the same short-wave behavior as Renardy because the curvature of the pipe disappears from the asymptotic equations. With surface tension they claim that the flow stabilizes at large enough k. Our results disagree with this conclusion.

Wilson and Rallison [11] generalized the UCM results to Oldroyd-B liquids, again with $k^{-1} \ll L$. They found that the addition of a Newtonian component to the viscosity has a destabilizing effect. In the limit where the Newtonian viscosity is large compared to the elastic stress, they found instability whenever the relaxation times of the two liquids are different. In the presence of surface tension at large enough k they showed that the normal force due to surface tension dominates the elastic normal force which suggests that the interface and hence the flow should be stabilized. However, we show that at large Wi the normal force balance is irrelevant to the stability.

We consider Couette flow through a channel of width L with walls moving at a relative velocity of U_0. In characterizing the different classes of interfacial instability it is important to recognize that for viscoelastic liquids in Couette flow three length scales enter the problem: the channel width L, the wavelength of the disturbance k^{-1}, and the relative distance $U_0\tau$ travelled by the walls in a relaxation time τ. This final length scale is a measure of the distance a typical particle travels during a relaxation time. Other length scales can be constructed from these three. For example liquid particles initially separated by the distance $2\pi L/U_0\tau k$ in the cross-stream (y) direction are separated by a wavelength in the streamwise (x) direction after a relaxation time. We find later that the length scale $L/U_0\tau k$ determines the thickness of boundary layers in the flow.

The previous analyses considered $k^{-1} \ll L$ (short-waves) or $k^{-1} \gg L$ (long-waves) and implicitly assumed that $k^{-1} \ll U_0\tau$ for short-waves or $k^{-1} \gg U_0\tau$ for long-waves. This leaves two other limits unexplored: $L \ll k^{-1} \ll U_0\tau$ and $U_0\tau \ll k^{-1} \ll L$. In the latter case the Weissenberg number $Wi = U_0\tau/L$ is small and the elastic effects are weak; the analysis of [1,5] for $k^{-1} \ll U_0\tau \ll L$ applies to this case. This paper focuses on the unexplored former case for which $Wi \gg 1$. In this regime the wavelength is long compared to the channel width, but short compared to the relaxation length scale. This leads to a mixture of short and long-wave properties, allowing us to use standard short-wave techniques, but also to make standard long-wave assumptions (e.g., the pressure gradient varies only in the x-direction).

The organization of this paper is as follows: In Section 2 we describe the governing equations and the unperturbed Couette flow. In Section 3 we study the large Wi limit of the UCM liquid analytically and numerically, and in Section 4 we study the large Wi limit of the Oldroyd-B liquid numerically. We then discuss the effect of surface tension, showing in Section 5 that even for moderate Wi some flows are not stabilized by arbitrarily large surface tension. In Section 6 we discuss the physical scalings of the instability. An additional instability is briefly analyzed in Section 7. In Section 8 we show that the main instability of this paper is robust in that it persists for other flow profiles under some mild assumptions. Finally, in Section 9 we offer some concluding remarks.

2. Governing equations

Consider two incompressible Oldroyd-B liquids in steady Couette flow in a channel of width L as shown in Fig. 1. We choose the origin in y to be the location of the unperturbed interface. The frame of reference is chosen to travel with the interface velocity. The lower liquid occupies a fraction Δ of the channel; the walls at $y = (1-\Delta)L$ and $y = -\Delta L$ move horizontally with velocity $(1-\Delta)U_0$ and $-\Delta U_0$ respectively.

The liquids have different relaxation times τ_- and τ_+ but the same, constant, shear viscosity μ, as well as the same relative contributions of elastic and Newtonian components to that viscosity. Without loss of generality we take $\tau_- \geq \tau_+$. In the absence of inertia we have

$$\nabla \cdot \Sigma = \mathbf{0}, \tag{1}$$

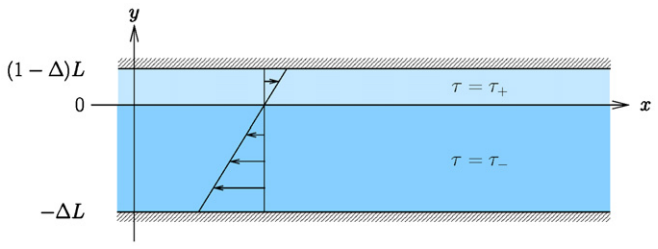

Fig. 1. Two elastic liquids in Couette flow $U = U_0 y/L$ through a channel. The liquids differ only in relaxation time τ.

Please cite this article in press as: J.C. Miller, J.M. Rallison, Interfacial instability between sheared elastic liquids in a channel, J. Non-Newtonian Fluid Mech. (2007), doi:10.1016/j.jnnfm.2007.01.009

$$\Sigma = -P\mathsf{I} + \mu\left(2\beta\mathsf{E} + \frac{1-\beta}{\tau}\mathsf{A}\right), \tag{2}$$

$$(\partial_t + \boldsymbol{U}\cdot\nabla)\mathsf{A} - [\nabla\boldsymbol{U}]^{\mathrm{T}}\cdot\mathsf{A} - \mathsf{A}\cdot[\nabla\boldsymbol{U}] = \frac{1}{\tau}(\mathsf{I}-\mathsf{A}), \tag{3}$$

$$\mathsf{E} = \frac{(\nabla\boldsymbol{U}) + (\nabla\boldsymbol{U})^{\mathrm{T}}}{2}, \tag{4}$$

$$\nabla\cdot\boldsymbol{U} = 0. \tag{5}$$

The stress tensor Σ depends on an elastic strain A. The shear viscosity μ, identical for both liquids, is divided into Newtonian and elastic parts through the parameter β, $0 \le \beta \le 1$. The value of β is also the same for both liquids. When $\beta = 0$ we have Upper Convected Maxwell (UCM) liquids, while when $\beta = 1$ the liquids are Newtonian. In the absence of a perturbation, the velocity is $\boldsymbol{U} = (U_0 y/L, 0)$.

The forces acting on the interface must balance, so

$$[\![\Sigma]\!]\cdot\boldsymbol{N} = \gamma\kappa\boldsymbol{N}, \tag{6}$$

where the notation $[\![\cdot]\!]$ denotes the jump in the bracketed quantity across the interface. $\boldsymbol{N}$ is the unit normal pointing into the upper liquid, γ the coefficient of surface tension and $\kappa = \nabla\cdot\boldsymbol{N}$ the curvature of the interface. For the base flow $\boldsymbol{N} = (0,1)^{\mathrm{T}}$.

In steady flow $(\partial_t + \boldsymbol{U}\cdot\nabla)\mathsf{A} = 0$ so Eq. (3) implies that the base elastic stress in each liquid is

$$\mathsf{A}_{\pm} = \begin{pmatrix} 2(U_0^2\tau_{\pm}^2/L^2) + 1 & U_0\tau_{\pm}/L \\ U_0\tau_{\pm}/L & 1 \end{pmatrix}.$$

This completes the definition of the base flow.

The linear perturbation equations for stability of modes proportional to $\exp(ikx - i\omega t)$ are derived in Appendix A and agree with those obtained in [11] with the addition of surface tension. We introduce a streamfunction ψ for the perturbation flow, and use lowercase letters to denote perturbations to their uppercase counterparts. The growth of the stresses is regulated by $\alpha = -i\omega + ikU + 1/\tau$ which incorporates the complex growth of the instability, advection by the base flow, and relaxation. We look for modes for which the streamfunction ψ is not identically zero (cf., [17,18] which show the existence of stress perturbations which do not affect the velocity field). The appropriate rescaling of these equations in the $Wi \gg 1$ limit differs from earlier treatments [1,5] and is described below.

In Appendix B, we derive general analytic solutions to the non-dimensionalized linear perturbation equations of Section 2.1, but these are found to be useful only in limiting cases. For more general parameter values we use numerical methods described in Appendix C.

2.1. Non-dimensionalization

We use asterisks to denote non-dimensional variables and choose a rescaling appropriate for $Wi \gg 1$.

The relevant length scales depend on elastic properties and so have no analogue in Newtonian flows. The length scale $U_0\tau_-$ measures the relative distance travelled by particles on opposite sides of the channel in a relaxation time. This is the most appropriate measure of distance in the x-direction and we take

$$k^* = U_0\tau_- k,$$
$$x^* = x/U_0\tau_-$$

For the cross-stream y-direction, liquid particles separated by $2\pi/kWi$ in the vertical are separated by a wavelength $2\pi/k$ in the horizontal after a relaxation time τ_-. So we define

$$y^* = Wi\ \ ky.$$

We rescale time with τ_- and so

$$\tau_-^* = 1, \qquad \tau_+^* = \xi = \frac{\tau_+}{\tau_-},$$

and without loss of generality $0 \le \xi \le 1$. The values of ω^* and α^* are now

$$\omega^* = \tau_-\omega,$$
$$\alpha_{\pm}^* = \tau_-\alpha_{\pm} = -i\omega^* + iy^* + 1/\tau_{\pm}^*.$$

It is convenient to non-dimensionalize ψ by

$$\psi^* = \psi k^2\tau_- = k^{*2}\frac{\psi}{U_0^2\tau_-},$$

in which case the interfacial perturbation δ is rescaled to

$$\delta^* = k\delta.$$

Note that the scaling of δ is different from that of x and y.

The pressure is rescaled by

$$p^* = \frac{Wi^{-3}p\tau_-}{\mu}.$$

The a_{ij} are already dimensionless, but in order to ensure that the scaled variables remain $\mathcal{O}(1)$ as $Wi \to \infty$ we set

$$a_{11}^* = Wi^{-3}a_{11},$$
$$a_{12}^* = Wi^{-2}a_{12},$$
$$a_{22}^* = Wi^{-1}a_{22}.$$

The capillary number is given by $\mathrm{Ca} = U_0\mu/\gamma$. We define the dimensionless surface tension coefficient by

$$\gamma^* = \mathrm{Ca}^{-1}Wi^{-3}.$$

When $Wi \to \infty$, $\gamma^* \to 0$ unless $\mathrm{Ca} \sim Wi^{-3}$.

We now drop the asterisks on the variables. The dimensionless flow profile is then as given in Fig. 2. The dimensionless

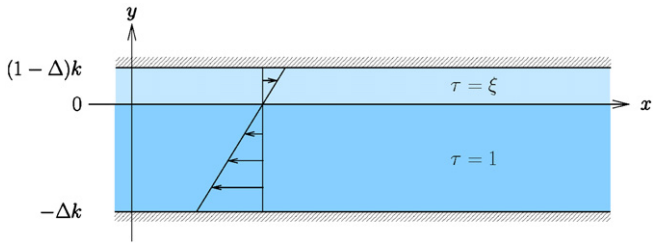

Fig. 2. The flow profile $U = y/k$ in non-dimensional variables. Without loss of generality $\xi \le 1$.

Please cite this article in press as: J.C. Miller, J.M. Rallison, Interfacial instability between sheared elastic liquids in a channel, J. Non-Newtonian Fluid Mech. (2007), doi:10.1016/j.jnnfm.2007.01.009

momentum equations (A.1) and (A.2) are now

$$i\left[-p+Wi^{-2}2\beta \mathrm{D}\psi+\frac{1-\beta}{\tau}a_{11}\right]+\mathrm{D}\left[\beta(\mathrm{D}^2+Wi^{-2})\psi+\frac{1-\beta}{\tau}a_{12}\right]=0, \tag{7}$$

$$i\left[\beta(\mathrm{D}^2+Wi^{-2})\psi+\frac{1-\beta}{\tau}a_{12}\right]+\mathrm{D}\left[-Wi^2p-2i\beta\mathrm{D}\psi+\frac{1-\beta}{\tau}a_{22}\right]=0, \tag{8}$$

where D denotes differentiation by y. The vorticity equation (A.3) becomes

$$\beta\left(\mathrm{D}^2-\frac{1}{Wi^2}\right)^2\psi+\frac{1-\beta}{\tau}\times\left[i\mathrm{D}\left(a_{11}-\frac{a_{22}}{Wi^2}\right)+\left(\mathrm{D}^2+\frac{1}{Wi^2}\right)a_{12}\right]=0, \tag{9}$$

where τ jumps at the interface. The constitutive equations (A.4)–(A.6) are

$$\alpha a_{11}=2a_{12}+2i(2\tau^2+Wi^{-2})\mathrm{D}\psi+2\tau\mathrm{D}^2\psi, \tag{10}$$

$$\alpha a_{12}=a_{22}+(2\tau^2+Wi^{-2})\psi+\mathrm{D}^2\psi, \tag{11}$$

$$\alpha a_{22}=2\tau\psi-2i\mathrm{D}\psi, \tag{12}$$

with $\alpha=-i\omega+iy+1/\tau$. The interfacial conditions (A.8)–(A.10) become

$$-2i(1-\beta)[\![\tau]\!]\delta+\beta[\![\mathrm{D}^2\psi]\!]+(1-\beta)\left[\!\left[\frac{a_{12}}{\tau}\right]\!\right]=0, \tag{13}$$

$$\left[\!\left[i\beta\mathrm{D}^3\psi+\frac{1-\beta}{\tau}\left(i\mathrm{D}a_{12}+\frac{a_{22}}{Wi^2}-a_{11}\right)\right]\!\right]=\gamma k\delta, \tag{14}$$

$$[\![\psi]\!]=0, \tag{15}$$

$$[\![\mathrm{D}\psi]\!]=0, \tag{16}$$

and the perturbed interface location is

$$\delta=\frac{\psi}{\omega}. \tag{17}$$

The no-slip boundary conditions (A.7) at the walls become

$$\psi=\mathrm{D}\psi=0 \quad \text{at} \quad y=(1-\Delta)k,-\Delta k. \tag{18}$$

The wall locations explicitly depend on k. The only other appearance of the wavenumber k is in the surface tension term in (14).

Eqs. (9)–(18) define the eigenvalue problem for $\omega=\omega(k,\xi,\beta,\Delta,Wi,\gamma)$. We are primarily interested in the large Wi limit. Examination of Eq. (9) shows that this is a regular limit, and that the error is $\mathcal{O}(Wi^{-2})$. This is made explicit in Appendix B. The coefficient of surface tension γ is negligibly small at large Wi unless $\mathrm{Ca}=\mathcal{O}(Wi^{-3})$.

2.1.1. Linear perturbation equations for $Wi \gg 1$

At leading order for large Wi, the momentum equations become

$$i\left(-p+\frac{1-\beta}{\tau}a_{11}\right)+\mathrm{D}\left[\beta\mathrm{D}^2\psi+\frac{1-\beta}{\tau}a_{12}\right]=0, \tag{19}$$

$$\mathrm{D}p=0. \tag{20}$$

The vorticity equation

$$\beta\mathrm{D}^4\psi+\frac{1-\beta}{\tau}[i\mathrm{D}a_{11}+\mathrm{D}^2a_{12}]=0 \tag{21}$$

can be exactly integrated once, the constant of integration being the x-dependent pressure gradient along the channel, and so the flow is governed by the x-momentum Eq. (19). This reflects the fact that the relaxation length scale is large compared to the channel width. The constitutive equations are

$$\alpha a_{11}=2a_{12}+4i\tau^2\mathrm{D}\psi+2\tau\mathrm{D}^2\psi, \tag{22}$$

$$\alpha a_{12}=a_{22}+2\tau^2\psi+\mathrm{D}^2\psi, \tag{23}$$

$$\alpha a_{22}=2\tau\psi-2i\mathrm{D}\psi. \tag{24}$$

The interfacial conditions become

$$-2i(1-\beta)[\![\tau]\!]\delta+\beta[\![\mathrm{D}^2\psi]\!]+(1-\beta)\left[\!\left[\frac{a_{12}}{\tau}\right]\!\right]=0, \tag{25}$$

$$\left[\!\left[i\beta\mathrm{D}^3\psi+\frac{1-\beta}{\tau}(i\mathrm{D}a_{12}-a_{11})\right]\!\right]=\gamma k\delta, \tag{26}$$

$$[\![\psi]\!]=0, \tag{27}$$

$$[\![\mathrm{D}\psi]\!]=0. \tag{28}$$

We keep the surface tension term for use in Section 5 where we consider the possibility that $\mathrm{Ca}=\mathcal{O}(Wi^{-3})$. Elsewhere we take $\gamma=0$. The displacement of the perturbed interface is

$$\delta=\frac{\psi}{\omega}, \tag{29}$$

and the no-slip boundary conditions at the walls remain

$$\psi=\mathrm{D}\psi=0 \quad \text{at} \quad y=(1-\Delta)k,-\Delta k. \tag{30}$$

3. UCM liquids ($\beta=0$) at high Weissenberg number

We first consider the UCM liquid neglecting surface tension ($\gamma=0$) and using Eqs. (21)–(30). This is the simplest case to study and has the fewest parameters. The solution for the streamfunction ψ has the particularly simple form

$$\psi(y)=C_1^{\pm}(y-\omega)+C_2^{\pm}y(y-\omega)+C_3^{\pm}e^{(-1-i)\tau_{\pm}y}+C_4^{\pm}e^{(1-i)\tau_{\pm}y}, \tag{31}$$

where $\pm$ denotes the solution on either side of the interface. The coefficients must be chosen to satisfy the no-slip boundary conditions at each wall as well as force balance and continuity of velocity at the interface. These eight equations are linear in the $C_i^{\pm}$. We find ω by the requirement that the associated matrix has determinant zero.

Please cite this article in press as: J.C. Miller, J.M. Rallison, Interfacial instability between sheared elastic liquids in a channel, J. Non-Newtonian Fluid Mech. (2007), doi:10.1016/j.jnnfm.2007.01.009

3.1. Asymptotic results for $Wi \gg k \gg 1$

When $Wi \gg k \gg 1$, we can calculate ω asymptotically.

The exponential terms in (31) have a length scale of order unity, but the walls are at asymptotically large distances of order k from the interface. In consequence, for the upper liquid ($y > 0$) the coefficient C_4^+ must be exponentially small. Thus the corresponding term must be negligible close to the interface. Similarly, the C_3^+ term is negligible close to the wall.

We now find C_2^+ in terms of C_1^+. As $k \to \infty$, the two boundary conditions at the wall $\psi = \mathrm{D}\psi = 0$ are satisfied by

$$C_1^+(y-\omega) + C_2^+ y(y-\omega) + C_4^+ e^{(1-i)\tau_+ y}$$

at $y = (1-\Delta)k \gg 1$. Some algebra shows that at leading order in k

$$C_1^+ = k(\Delta - 1)C_2^+.$$

A similar argument gives

$$C_1^- = k\Delta C_2^-.$$

Since $k \gg 1$, we conclude that the $C_2^\pm$ are much smaller than the $C_1^\pm$.

Applying the interfacial conditions (25)–(29) at $y = 0$ and neglecting the exponentially small terms involving C_3^- and C_4^+, we find $\mathsf{M}\,\boldsymbol{v} = 0$ where $\boldsymbol{v} = [C_1^-, C_4^-, C_1^+, C_3^+]^{\mathrm{T}}$ and

$$\mathsf{M} = \begin{pmatrix} 0 & 2\dfrac{\omega^2+2i\omega+\omega+i}{\omega(\omega+i)^2} & 0 & 2\xi\dfrac{\xi^2\omega^2+2i\xi\omega-\xi\omega-i}{\omega(\xi\omega+i)^2} \\ -\dfrac{2}{\Delta} & 0 & \dfrac{2\xi}{\Delta-1} & 0 \\ 1 & (1-i) & -1 & (1+i)\xi \\ -\omega & 1 & \omega & -1 \end{pmatrix}, \tag{32}$$

to leading order in k. The first and second rows of M arise from the x- and y-components of the force balance while the third and fourth rows come from the x- and y-components of continuity of velocity.

We seek ω such that $\det\mathsf{M} = 0$. We replace the fourth row of M with the sum of the fourth row and ω times the third row. The rows of the resulting matrix are linearly dependent if and only if the first and (new) fourth rows are linearly dependent. That is, $\det\mathsf{M} = 0$ if and only if $\det\mathsf{N} = 0$ where

$$\mathsf{N} = \begin{pmatrix} 2\dfrac{\omega^2+2i\omega+\omega+i}{\omega(\omega+i)^2} & 2\xi\dfrac{\xi^2\omega^2+2i\xi\omega-\xi\omega-i}{\omega(\xi\omega+i)^2} \\ 1+\omega(1-i) & -1+\omega\xi(1+i) \end{pmatrix}. \tag{33}$$

The combination of terms used to give the second row of N represents continuity of the material derivative of the x-component of velocity at the interface, that is, continuity of tangential acceleration at the interface. The flow generated by $\psi = C_1^\pm(y-\omega)$ has the property that the x-component of velocity for a material particle does not change: the Eulerian derivative at a point is balanced by the change in the base flow due to advection in the y-direction. Consequently the coefficients $C_1^\pm$ cancel exactly and do not appear in the second row of N. They similarly drop out of the tangential force balance and thus do not affect the condition for stability. It is only the two terms that decay exponentially away from the interface (C_4^- and C_3^+) that appear in the reduced pair of tangential interfacial conditions.

After some algebra the determinant of N yields the quintic equation:

$$\begin{aligned} 2\xi^3\omega^5 &+ (\xi^3 + 4i\xi^3 - \xi^2 + 4i\xi^2)\omega^4 + (-2\xi^3 - 8\xi^2 - 2\xi)\omega^3 \\ &+ (-2\xi - i\xi^3 - 3i\xi^2 - 3i\xi - i + 2\xi^2)\omega^2 \\ &+ (2\xi^2 - 2\xi + \xi^2 i + 2 - i)\omega - \xi + 1 = 0. \end{aligned} \tag{34}$$

This is identical to the large Wi limit of Renardy's result [1] which assumes the perturbations decay before reaching the wall. This is a remarkable conclusion, for it implies that the growth rate of the instability is unaffected by the presence of the channel walls even though the mode structure is changed.

The neutral stability boundary occurs when ω is real. The only ξ allowing real ω are $\xi = 1$ and $\xi = \xi_c \approx 0.27688$. Between these values the imaginary part of ω is positive, and below this range it is negative. The imaginary and real parts of the most dangerous root for ω are plotted in Fig. 3.

For $\xi = 0.5$, Eq. (34) gives $\omega \approx -.30544 + .06603i$. Thus at large k we expect an instability with growth rate $0.06603 + \mathcal{O}(1/k)$ and wavespeed $-0.30544/k + \mathcal{O}(1/k^2)$. Both limits are clear in Fig. 4 where we have solved the problem numerically with $\xi = 0.5$, $\Delta = 0.7$ for arbitrary k. For moderate k, the growth rate overshoots the asymptote but decreases again at large k. Fig. 5 shows the corresponding perturbation flow at $k = 30$ which occupies the full width of the channel with boundary layers at the interface and the wall.

Our observations for $Wi \gg k \gg 1$ can be summarized as follows: we have found an algebraic equation for ω which gives the stability boundary in terms of ξ, the ratio of relaxation times. The perturbation flow is of comparable magnitude throughout the channel, with boundary layers at the walls and at the interface. The stability criterion is unaffected by the walls and can be expressed in terms of velocities and forces that are parallel to the interface.

3.2. Stability for $Wi \gg 1$ and general k

To illustrate the stability boundary for general k, we fix ξ and allow Δ and k to vary. Fig. 6 shows the marginal sta-

Please cite this article in press as: J.C. Miller, J.M. Rallison, Interfacial instability between sheared elastic liquids in a channel, J. Non-Newtonian Fluid Mech. (2007), doi:10.1016/j.jnnfm.2007.01.009

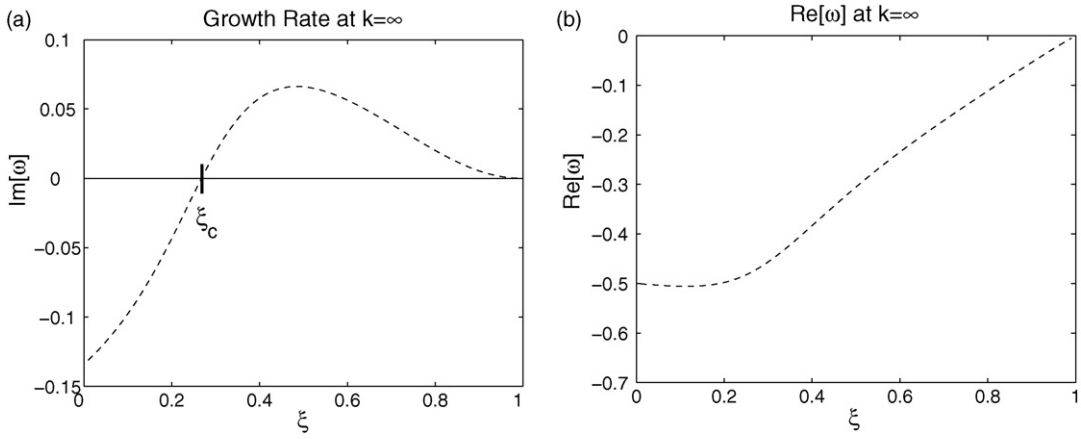

Fig. 3. UCM liquid. $Wi \gg k \gg 1$. Imaginary and real parts of ω for Eq. (34) as ξ changes. (a) Growth rate. (b) Real part of ω.

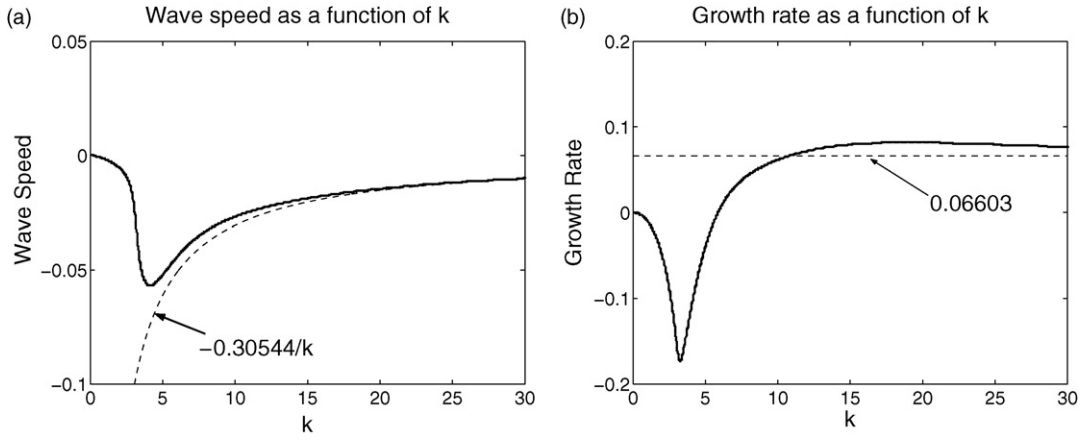

Fig. 4. UCM liquids. $Wi \gg 1$ for varying k. Growth rates and wave speeds calculated from (19)–(30) compared with the $Wi \gg k \gg 1$ asymptotic predictions (dashed) for $\xi = 0.5$, $\Delta = 0.7$. (a) Wave speed. (b) Growth rate.

bility curves in (k, Δ) space. For $k \ll 1$ the wavelength is long compared to both the channel width and the relaxation length scale, so this is a special case of previous long-wave analysis [10] with instability if $\Delta < 0.5$. If $\xi > \xi_c \approx 0.28$ we have shown there is an instability for $k \gg 1$. This is clear in Fig. 6. For $\xi < \xi_c$, there is an unstable tongue for moderate k which grows as $\xi \to \xi_c$, filling most of the plot for $\xi = 0.2$.

The overshoot in Fig. 4 and the unstable 'tongues' in Fig. 6(a) and (b) both show that the growth rate overshoots the large k prediction when k is moderate. This suggests that the next correction in k for $k \gg 1$ is destabilizing.

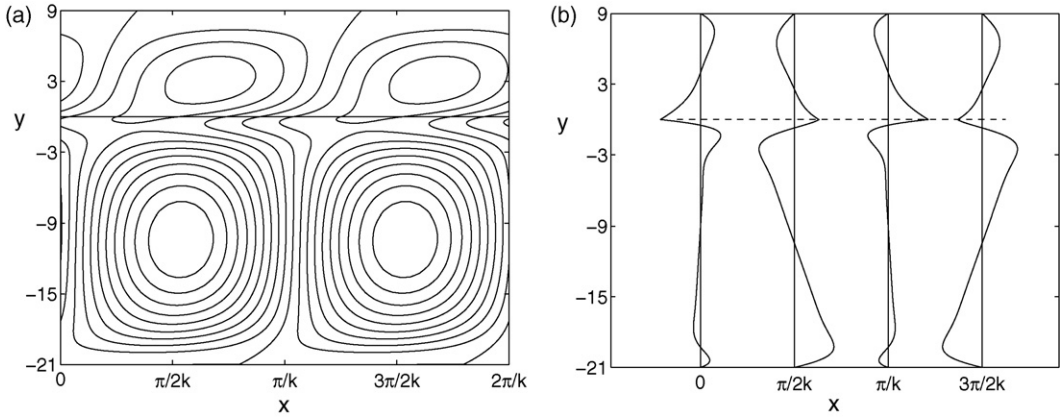

Fig. 5. UCM liquids. $Wi \gg 1$. Unstable mode for $\xi = 0.5$, $\Delta = 0.7$, and $k = 30$. The value of ω is $-0.3000 + 0.0766i$. There are boundary layers close to the interface and the walls. The magnitude of the flow is comparable throughout the channel. (a) Streamlines. (b) Perturbed x-velocity. Note the boundary layers at the interface and both walls.

Please cite this article in press as: J.C. Miller, J.M. Rallison, Interfacial instability between sheared elastic liquids in a channel, J. Non-Newtonian Fluid Mech. (2007), doi:10.1016/j.jnnfm.2007.01.009

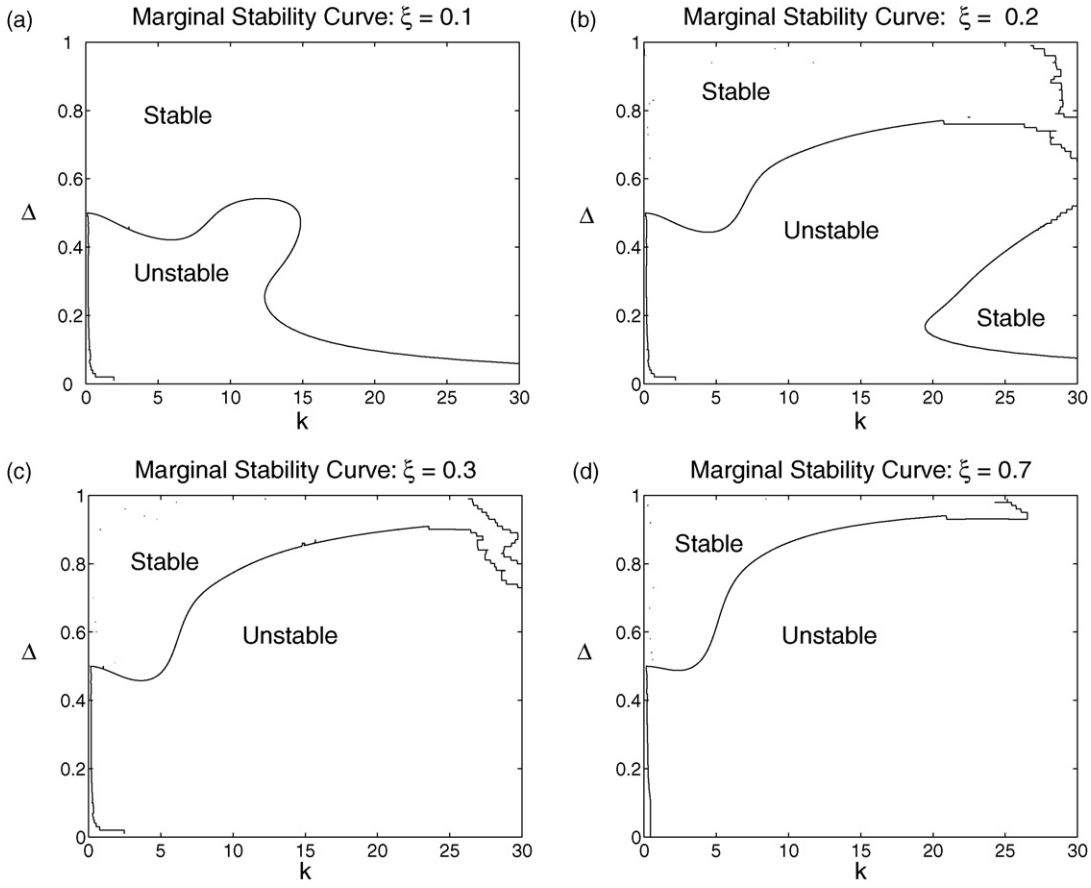

Fig. 6. UCM liquids. $Wi \gg 1$. Marginal stability curves in Δ-k space at fixed values of ξ. The noisy areas for large k or small Δ correspond to regions of numerical difficulties. (a) $\xi = 0.1$. Well below ξ_c, short-waves are stable. There is a small unstable tongue at $10 \lesssim k \lesssim 15$. (b) $\xi = 0.2$. Just below ξ_c short-waves are stable, but the unstable tongue has grown much larger. (c) $\xi = 0.3$. Just above ξ_c, short-waves are unstable and the instability persists down to $k \approx 5$. (d) $\xi = 0.7$. The picture is largely unchanged from $\xi = 0.3$.

4. Oldroyd-B liquids ($\beta > 0$) for $Wi \gg k \gg 1$

We consider here whether the $Wi \gg k \gg 1$ interfacial instability found for UCM liquids persists for Oldroyd-B liquids. By the similarities of the analytic solution with that of the UCM liquid, we are able to draw some similar conclusions about the mechanism of instability. However, to determine the growth rates, we find numerical methods more useful.

Because the term $C_1(y - \omega)$ remains part of solution (B.3) even in the presence of Newtonian viscosity the remarkable conclusion that C_1 drops out of the tangential force and tangential acceleration condition at the interface remains valid regardless of β. We expect that C_2 is small in order to satisfy boundary conditions at the wall, and so the algebraic terms disappear and the stability is determined entirely by the two tangential conditions in the interfacial boundary layer.

Wilson and Rallison [11] studied the $k \gg 1$ limit for Oldroyd-B liquids with moderate Wi. In this limit the perturbation flow decays away from the interface and the walls can be neglected. They showed that for sufficiently large β there is instability for all ξ, with the growth rate tending to zero like $(1 - \beta)^3$ as β increases to 1. It is known from the UCM results of Renardy [1] that for sufficiently large Wi (but still small compared to k) there are values of ξ for which the flow is stable if $\beta = 0$. These results suggest the existence of a critical value of β above which all flows are unstable. Wilson and Rallison were able to find stability for β as large as 0.11, and postulated that this is the critical value. When Wi is larger than k, their analysis breaks down because the walls lie within the boundary layer. Asymptotics become difficult. We have investigated this using numerics instead, with the governing Eqs. (21)–(30).

Setting $\Delta = 0.5$ we fix $k = 30$, 60, and 120 and follow the growth rate in (β, ξ) space in Fig. 7. At $k = 30$, there is stability if both ξ and β are small, shown in Fig. 7(a). As k grows, the stable region increases in size and exists for β up to (at least) 0.2.

In the limit $\beta \to 1$, the liquids become identical Newtonian liquids and so the growth rate tends to zero. That is, for fixed k, $\lim_{\beta\to 1} \Im[\omega] = 0$. However, it is clear from the figures that $\lim_{\beta\to 1}\lim_{k\to\infty} \Im[\omega] \neq 0$: the limit is singular. This is different from the $Wi \ll k$ case in [11].

To observe the structure of the unstable mode when the liquids are almost Newtonian, we take $\xi = 0.5$, $\Delta = 0.7$, $\beta = 0.99$, and $k = 2000$. The perturbation flow is shown in Fig. 8. The boundary layers at the wall have effectively disappeared. There are still boundary layers close to the interface, but their structure has changed.

Please cite this article in press as: J.C. Miller, J.M. Rallison, Interfacial instability between sheared elastic liquids in a channel, J. Non-Newtonian Fluid Mech. (2007), doi:10.1016/j.jnnfm.2007.01.009

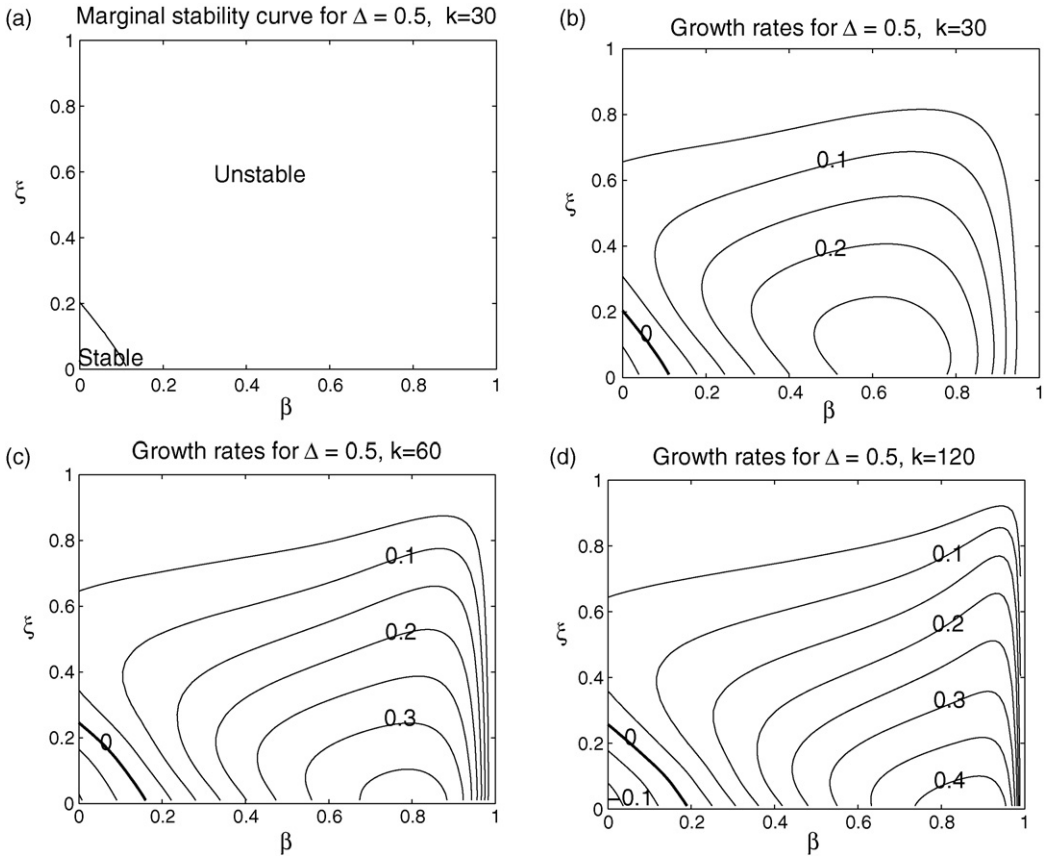

Fig. 7. Growth rate contours in the (β, ξ) plane for Oldroyd-B liquids with $Wi \gg 1$ and $\Delta = 0.5$ for $k = 30$, 60, and 120. The lower left corner is the only region of stability. If either $\xi = 1$ or $\beta = 1$, the two liquids are identical, and the growth rate is zero. For $\beta = 0$ (UCM) the $k \gg 1$ asymptotic results from Eq. (34) are in good agreement. (a) The marginal stability curve at $k = 30$. (b) The growth rate at $k = 30$. (c) The growth rate at $k = 60$. (d) The growth rate at $k = 120$.

Our results show that the behavior of Oldroyd-B fluids is similar to that of UCM fluids. The critical value of β at which stability is impossible appears to be approximately 0.2. We have found that the $\beta \to 1$ and $k \to \infty$ limits cannot be interchanged.

5. The effect of surface tension

Insofar as an elastic instability requires a displacement of the interface, surface tension will be expected to suppress the instability, especially for large k. However, in this section we find that surface tension does not eliminate instabilities, and so the mechanism of the instability does not require a perturbation to the interface.

5.1. The effect of surface tension at high Weissenberg number

In this section we assume that $\mathrm{Ca} \sim Wi^{-3}$ so that surface tension remains dynamically important at large Wi.

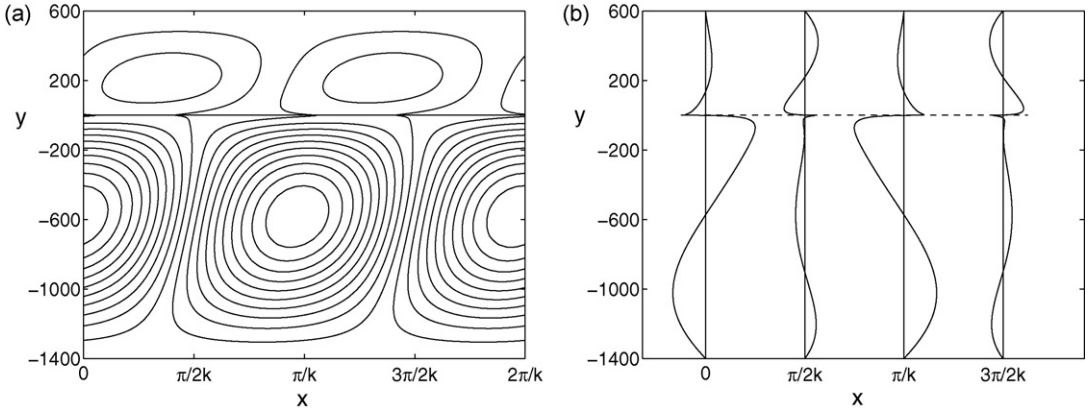

Fig. 8. Unstable perturbation flow of Oldroyd-B liquid with $Wi \gg 1$, $\beta = 0.99$, $\xi = 0.5$, $\Delta = 0.7$, and $k = 2000$. For these parameters $\omega = -0.0261 + 0.3330i$. Compare with Fig. 5 where $\beta = 0$, $\Delta = 0.7$, $k = 30$, and $\xi = 0.5$. (a) Streamlines. (b) Perturbed x-velocity.

Please cite this article in press as: J.C. Miller, J.M. Rallison, Interfacial instability between sheared elastic liquids in a channel, J. Non-Newtonian Fluid Mech. (2007), doi:10.1016/j.jnnfm.2007.01.009

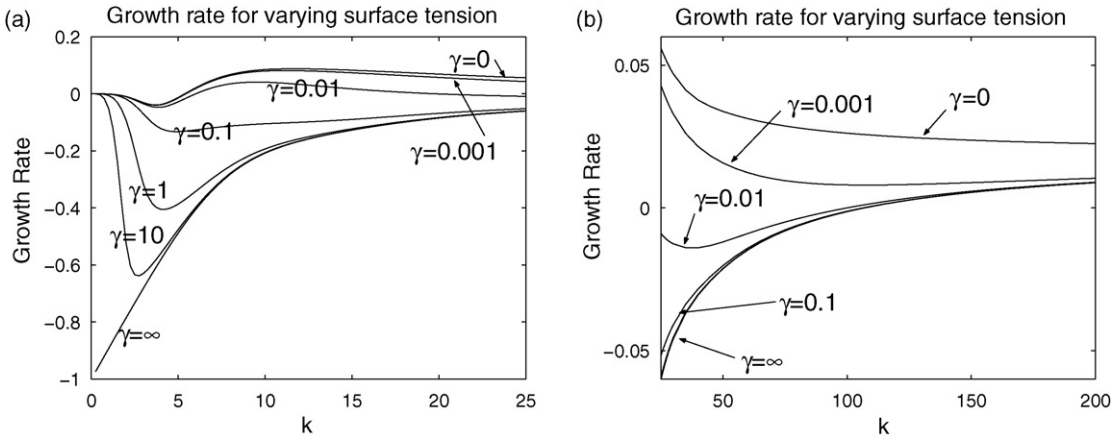

Fig. 9. UCM liquids. The effect of surface tension on growth rate for $Wi \gg 1$, $\xi = 0.3$, and $\Delta = 0.5$. For $k \gg 1$ all growth rates tend to the asymptotic limit 0.019. (a) $0 < k < 25$. (b) $25 < k < 200$.

We consider Eqs. (21)–(30), with $\gamma \neq 0$. In the limit $k\gamma \to \infty$, the normal force balance (26) reduces to $\delta = 0$. Since $\delta = 0$, the kinematic equation for the interface (29) becomes $\psi(0) = 0$ and δ disappears from the problem. The only remaining time derivatives are in the evolution of the stress perturbation, Eqs. (22)–(24). Thus any instability manifests itself only in the growth of the liquid velocity and elastic stresses and not in an interfacial perturbation.

5.1.1. UCM liquids ($\beta = 0$) with nonzero surface tension

In the limit where $Wi \gg k \gg 1$, we have a simple analytic representation of the streamfunction in both liquids, and we proceed as in Section 3.1. The addition of surface tension affects only the second row of the matrix M in Eq. (32). This row plays no role in the construction of N in Eq. (33), and so the linear stability of the system is unchanged by the addition of surface tension (although the perturbation flow is changed). The remarkable conclusion is that a perturbation with the same growth rate occurs regardless of the size of the surface tension whenever $Wi \gg k \gg 1$.

To see the effect of surface tension at moderate k we solve the equations numerically. In Fig. 9 we plot the growth rates with $\xi = 0.3$ and $\Delta = 0.5$ for different values of the surface tension measured by γ. The infinite surface tension ($\gamma = \infty$) curve was calculated by replacing the normal force balance with the zero-displacement condition $\psi(0) = 0$. As expected, the growth rate of the disturbance is everywhere reduced by the addition of surface tension. For small k the growth rates are close to the zero surface tension limit. As k increases, they approach the infinite surface tension limit. However as $k \to \infty$, both zero and infinite surface tension limits tend to the same (positive) growth rate, 0.019.

In Fig. 10 we show the perturbation flow for the same parameters as in Fig. 5 except that the surface tension is infinite. Boundary layers exist at the interface with the same length scale as before.

The fact that surface tension does not affect the growth rate if $Wi \gg k \gg 1$ has consequences for our understanding of the physical mechanism driving the $k \gg 1$ instability. At large Wi the mechanism cannot depend on interface displacement, contradicting previous claims [9,20], instead it must rely on effects tangential to the interface that are not affected by surface tension. We do not have a physical explanation for the instability mechanism, but it seems depen-

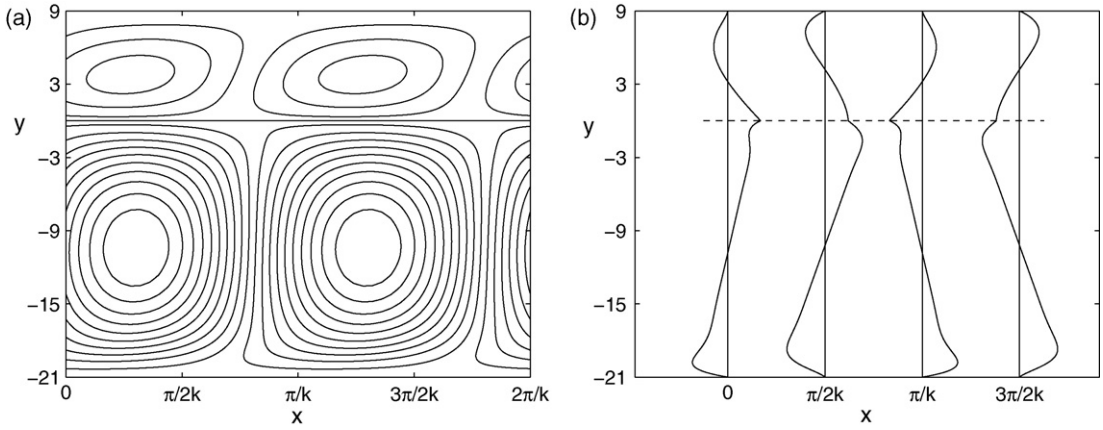

Fig. 10. UCM liquids. Perturbation flow for the same parameters as in Fig. 5: $Wi \gg 1$, $\xi = 0.5$, $\Delta = 0.7$, and $k = 30$, but with $\gamma = \infty$. The value of ω is $-0.2855 - 0.0227i$. As k increases it destabilizes and tends to the same growth rate as for the zero surface tension case. (a) Streamlines at infinite surface tension. The interface is flat. (b) Perturbed x-velocity.

Please cite this article in press as: J.C. Miller, J.M. Rallison, Interfacial instability between sheared elastic liquids in a channel, J. Non-Newtonian Fluid Mech. (2007), doi:10.1016/j.jnnfm.2007.01.009

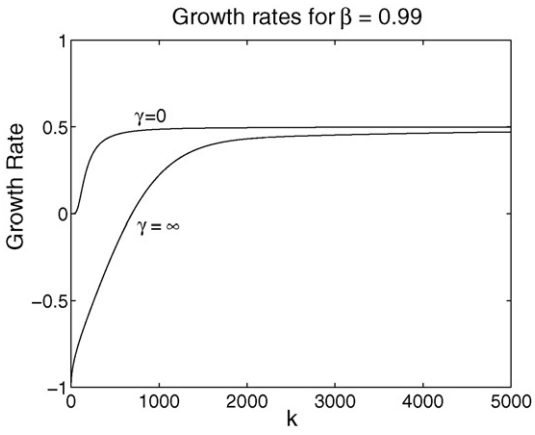

Fig. 11. Oldroyd-B liquids with $Wi \gg 1$. Plot of growth rates for $\beta = 0.99$ as k changes with $\xi = 0.1$ and $\Delta = 0.5$ fixed. The top curve corresponds to zero surface tension, while the bottom curve assumes it is infinite so that the interface remains flat.

dent on base advection of perturbed stresses combined with relaxation.

5.1.2. *Oldroyd-B liquids ($\beta > 0$) with nonzero surface tension at high Weissenberg number*

We have not undertaken a complete study of parameter space for Oldroyd-B liquids with surface tension, but because tangential effects determine the stability of Oldroyd-B liquids at large *Wi*, we expect surface tension to have no influence at sufficiently large *k*.

In Fig. 11 we plot the growth rates for $\xi = 0.1$, $\Delta = 0.5$, and $\beta = 0.99$. We see that the infinite surface tension growth rate is positive for $k \gg 1$, and appears in this limit to approach the same value as for zero surface tension.

5.2. *The effect of surface tension for UCM liquids at general Wi and $k \gg 1$*

Setting $Wi = \mathcal{O}(1)$ and $k \gg 1$ corresponds to a disturbance wavelength that is much shorter than both the channel width and the relaxation length. This is the standard short-wave limit, which has been studied in the absence of surface tension by Renardy [1] and Chen and Joseph [5].

In the presence of surface tension, Chen and Joseph [5] state that at sufficiently large *k* the flow is stable. This contrasts with our results at asymptotically large *Wi*. To explore this discrepancy, we consider the effect of surface tension at finite *Wi*. We first reproduce the results of [1,5] without surface tension and then consider the infinite surface tension limit.

With moderate *Wi* in the absence of surface tension, the walls become irrelevant for $k \gg 1$ and *k* disappears from the analysis. The solution from (B.2) is a sum of exponentially growing and decaying terms. The growing terms must vanish, so the solutions take the form

$$\psi(y) = C_1^-(y-\omega)\exp\left(\frac{y}{Wi}\right) + C_4^- \exp\left[\xi y\left(-i+\sqrt{1+\frac{1}{\xi^2 Wi^2}}\right)\right] \quad y<0,$$

$$\psi(y) = C_2^+(y-\omega)\exp\left(\frac{-y}{Wi}\right) + C_3^+ \exp\left[y\left(-i-\sqrt{1+\frac{1}{Wi^2}}\right)\right] \quad y>0.$$

The interfacial conditions with zero surface tension define a 4×4 matrix. Setting the determinant to zero provides a (complicated) quintic equation in ω found by Renardy [1] which reduces to Eq. (34) at large *Wi*. Fig. 12(a) plots the growth rate of the most dangerous mode in (Wi, ξ) space, equivalent to Fig. 1 of Chen and Joseph [5] and Fig. 1 of Renardy [1], but with different axis scalings.

In the case of infinite surface tension, we replace the normal force balance by $\psi(0) = 0$. Then the same method gives a (significantly simpler) quintic equation for ω:

$$([R\xi^3 + \xi^2 Q]Wi - i\xi^2 Q + iR\xi^2)\omega^5 + ([2i\xi^2 Q + 2iR\xi^3 + 2iR\xi^2 - \xi^2 + \xi^3 + 2i\xi Q]Wi + 2i\xi^2 - 2R\xi^2 + 2\xi^2 Q + 2\xi Q - 2R\xi)\omega^4$$

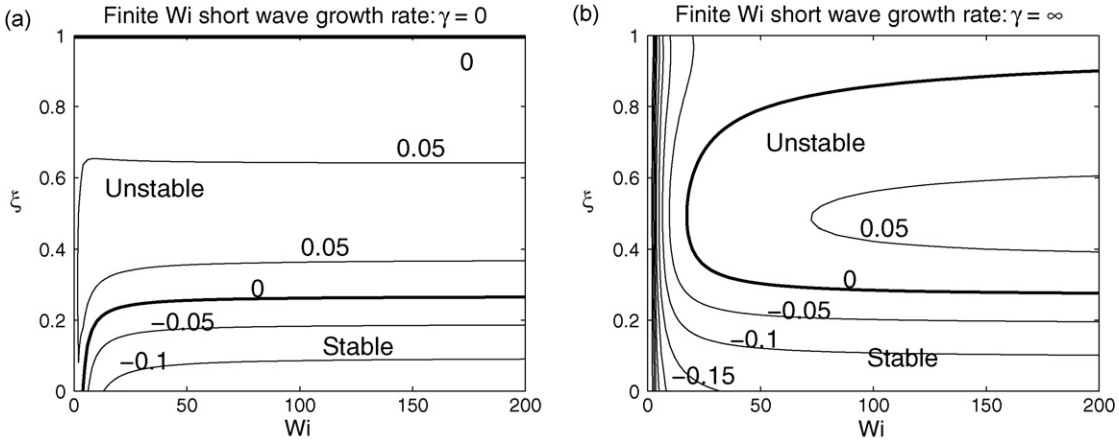

Fig. 12. UCM liquids. The effect of surface tension on the large *k* growth rate for finite *Wi*. As $Wi \to \infty$, the growth rates for zero and infinite surface tension coincide. (a) Growth rate contours with no surface tension. At $\xi = 1$ the growth rate is zero. (b) growth rate contours with infinite surface tension. The growth rate tends to -1 (i.e., pure relaxation) as $Wi \to 0$.

Please cite this article in press as: J.C. Miller, J.M. Rallison, Interfacial instability between sheared elastic liquids in a channel, J. Non-Newtonian Fluid Mech. (2007), doi:10.1016/j.jnnfm.2007.01.009

$$+\left([-2\xi^2 Q - iR\xi^2 Q - 4R\xi^2 - 2R\xi - i\xi + iRQ - 4\xi Q + i\xi^3]Wi + 2i\xi^2 Q - 4iR\xi - 3\xi^2 + 4i\xi Q - 3\xi - \xi^3 - 2iR - 1 + \frac{i - i\xi^2}{Wi}\right)\omega^3 + \left([iQ + iR\xi^2 - iR - 4iR\xi - i\xi^2 Q - 2RQ + 2R\xi Q - 4i\xi Q]Wi - 4i\xi^2 - 4i\xi + 4R - 4i - 4\xi Q + \frac{2\xi - 2}{Wi}\right)\omega^2 + ([-R\xi + 2\xi Q - Q + i\xi^2 + 2R - i]Wi - iQ + 4 + iR + 4\xi)\omega + [1 - \xi]Wi + 2i = 0,$$

where $Q = \sqrt{\xi^2 + 1/Wi^2}$ and $R = \sqrt{1 + 1/Wi^2}$. At leading order for $Wi \gg 1$ this also reduces to Eq. (34). On solving this quintic for finite Wi we find a region of parameter space where the system is *unstable*, seen in Fig. 12(b). As Wi increases, Fig. 12(a) and (b) become identical.

The fact that instability persists, with a growth rate of order unity, even with infinite surface tension contradicts the conclusions of Chen and Joseph [5], where it is assumed that the instability is caused by displacement of the interface. This assumption leads to an inappropriate ansatz that the stabilizing effect of surface tension on the growth rate is $\mathcal{O}(k)$ for $k \gg 1$, and hence an incorrect conclusion (at large Wi) that surface tension stabilizes the flow.

The fact that the instability exists with a flat interface further raises the possibility that the interaction between the liquid and the wall could also lead to an instability. However, the wall provides different boundary conditions, and earlier work [14] shows that instability does not occur.

6. Scalings of high *Wi* instabilities

Figs. 5, 8, and 10 show that the perturbation flow in the bulk of the liquids is as large as in the boundary layer close to the interface. In addition, we have seen that the growth rate of the instability is independent of the position of the walls.

This implies that the instability arises at the interface and that the remainder of the flow, whether in the bulk or the wall boundary layers, has no effect on the growth rate. In this section we offer a discussion of the scalings to explain why the outer region is dynamically passive despite having a flow of comparable magnitude.

6.1. The UCM liquid

For clarity and simplicity we focus on the infinite surface tension limit of the UCM liquids for which $\psi = 0$ at the interface and $\beta = 0$.

Because the wavelength is long compared with the channel width, the perturbation liquid velocity is parallel to the channel walls at leading order, the liquid pressure is constant across the channel, and the y-component of the momentum Eq. (20) is automatically satisfied. The x-component of the momentum Eq. (19) becomes

$$a_{11} - i\mathrm{D}a_{12} = G, \tag{35}$$

where D denotes differentiation in y, $G = p\tau$ is a perturbation pressure gradient, and a_{ij} is the perturbation to the ij component of the stress.

The evolution of the perturbation stresses in Eqs. (22)–(24) is controlled, through α, by the base flow advection y, growth ω, and relaxation τ^{-1}. In the boundary layer at the interface $y = \mathcal{O}(1)$. Outside the boundary layer $y = \mathcal{O}(k)$. It follows that $\alpha = -i\omega + ik + 1/\tau = \mathcal{O}(1)$ in the boundary layer and thus $a_{ij} \sim \psi$, but outside the boundary layer $\alpha = \mathcal{O}(k)$ and $|a_{ij}| \ll |\psi|$.

By Eq. (35), outside the interfacial boundary layer the pressure gradient G must be at most comparable to a_{11} and a_{12}. In the boundary layer the stresses are larger and the pressure is negligible, so Eq. (35) is a third-order ordinary differential equation having three solutions. We find $\mathrm{D} \sim 1$. One solution grows unphysically and is discarded, leaving two solutions whose coefficients can be chosen. The y-velocity is zero at the interface to satisfy the infinite surface tension assumption. The x-velocity may be fixed arbitrarily, so defining the magnitude of the perturbation. These two conditions uniquely determine ψ throughout the interfacial boundary layer.

The solutions in the bulk are algebraic and $\mathrm{D} \sim 1/y$. At the edge of the boundary layer, the x-velocity must be of comparable magnitude to that in the interior of the boundary layer. The flux of liquid in the x-direction in the boundary layer is negligible, so to conserve mass, the bulk region must have no net flux, but it must simultaneously match the x-velocity set by the boundary layer at its edge. The pressure gradient G is determined so as to maintain zero flux in the bulk, and so the horizontal flow throughout the bulk region is comparable to that in the boundary layer.

At the wall the flow must satisfy the no-slip boundary condition. This forces the existence of a second boundary layer, where again $\mathrm{D} \sim 1$. There is no appreciable flux in this layer.

In this scenario there is no feedback whereby the flow in the bulk can influence the flow in the interfacial boundary layer. Thus the growth rate is locally determined and the bulk flow is driven by this interfacial region.

6.2. The effect of β

Including Newtonian viscosity modifies the x-momentum equation so that it becomes

$$a_{11} - i\mathrm{D}a_{12} - i\frac{\beta\tau}{(1-\beta)}\mathrm{D}^3\psi = G. \tag{36}$$

The structure in each region begins to be affected by the β terms when: $\beta/(1-\beta) \sim 1$ in the interfacial boundary layer, $\beta/(1-\beta) \sim k$ in the bulk, and $\beta/(1-\beta) \sim 1/k$ in the wall boundary layer. Thus at sufficiently large k, the wall boundary layer is affected by the Newtonian viscosity, but the bulk flow is unchanged and the interfacial boundary layer is affected only if β is large enough. Because the bulk region is unchanged, it

Please cite this article in press as: J.C. Miller, J.M. Rallison, Interfacial instability between sheared elastic liquids in a channel, J. Non-Newtonian Fluid Mech. (2007), doi:10.1016/j.jnnfm.2007.01.009

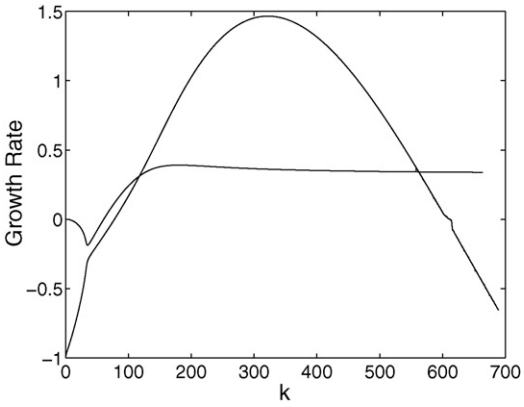

Fig. 13. High *Wi* growth rates for Oldroyd-B liquids with $\beta = 0.99$, $\xi = 0.5$, and $\Delta = 0.7$.

does not feed back into the interfacial layer and so the stability is again determined by the interfacial boundary layer.

The structure shown in Fig. 8 ($\beta = 0.99, k = 2000$) suggests that as $\beta \to 1$ the wall boundary layer expands until it has the same length scale as the bulk region.

7. An additional instability of Oldroyd-B liquids at high *Wi*

The picture we have developed so far for high *Wi* instabilities is incomplete. We have found (by accident) an additional instability in Oldroyd-B liquids. In this section we briefly analyze some of its properties.

In Fig. 13 we plot the growth rates for two unstable modes for $\beta = 0.99$, $\xi = 0.5$, and $\Delta = 0.7$. As $k \to \infty$ one of the modes has fixed growth rate. This is the previously observed mode discussed in Section 4. The other mode has higher growth rate at intermediate values of k, but stabilizes as $k \to \infty$.

We have not studied this new mode in detail. The perturbation flow for $k = 200$ is shown in Fig. 14. The real part of ω has a different sign from that of the $k \to \infty$ instability, and so this mode travels in the opposite direction of the $k \to \infty$ mode relative to the interface.

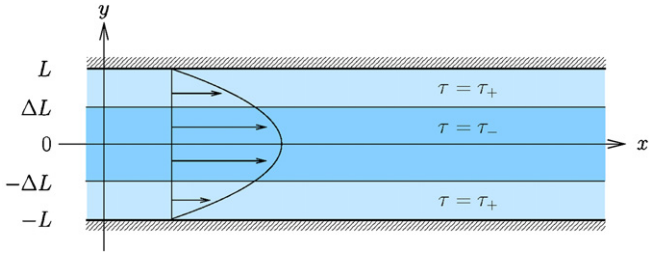

Fig. 15. Sketch for 'coextrusion' Poiseuille flow $U = U_0(1 - y^2/L^2)$ in a channel.

This mode stabilizes at large k, but the value of k at which it stabilizes increases as the interface approaches the wall. This suggests an interaction of the boundary layer at the interface with the wall. We have not found a similar instability in UCM flows, but we cannot rule out such a possibility.

8. Other flow profiles for the UCM liquids

We have shown that the large k instability in Couette flow is generated by effects close to the interface, even though the mode structure is influenced by the presence of the channel walls. Consequently, we expect to see unstable modes having the same growth rates for other base flow profiles whenever the Weissenberg number based on the local shear rate U' at the interface is sufficiently high. We demonstrate this by considering two cases of Poiseuille flow of two liquids through a channel.

We return to dimensional variables and consider two configurations. The first is symmetric three-layer Poiseuille flow (a 'coextrusion flow') as sketched in Fig. 15. We take the interfaces to be at $y = \pm\Delta L$. The second configuration is asymmetric; it has only two liquid layers with a single interface at $y = \Delta L$ so that $\tau = \tau_+$ for $\Delta < y/L < 1$ and $\tau = \tau_-$ for $-1 < y/L < \Delta$. In both cases, the base flow is $\boldsymbol{U} = (U(y), 0)$ where $U(y) = U_0(1 - y^2/L^2)$. The inner (lower) relaxation time is taken to be τ_- while the outer (upper) relaxation time is $\tau_+ = \xi\tau_-$. We neglect surface tension.

When the local Weissenberg number at the interface $U'\tau_- = 2U_0\Delta\tau_-/L$ is large we expect to see the same growth rate as found for Couette flow so long as the shear rate is effectively

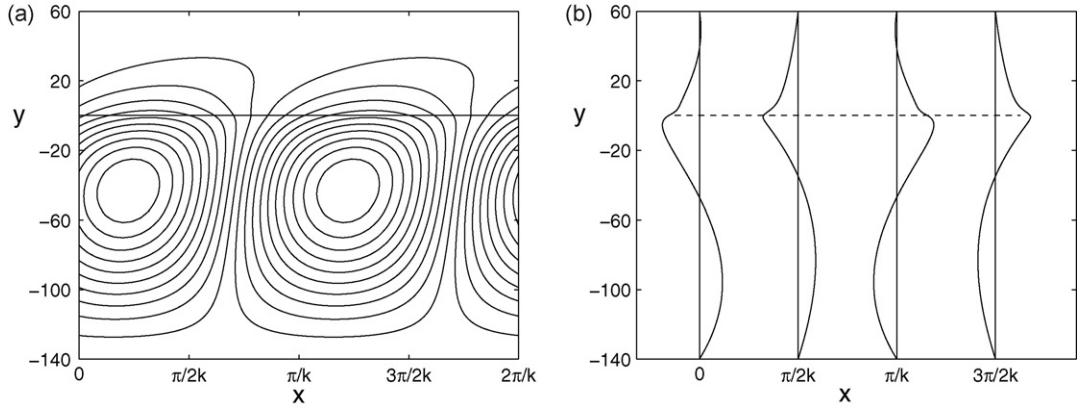

Fig. 14. Unstable high *Wi* perturbation flow of Oldroyd-B liquids with $\beta = 0.99$, $\xi = 0.5$, $\Delta = 0.7$, and $k = 200$. For these parameters $\omega = 1.6084 + 1.0262i$. (a) Streamlines. (b) Perturbed x-velocity.

Please cite this article in press as: J.C. Miller, J.M. Rallison, Interfacial instability between sheared elastic liquids in a channel, J. Non-Newtonian Fluid Mech. (2007), doi:10.1016/j.jnnfm.2007.01.009

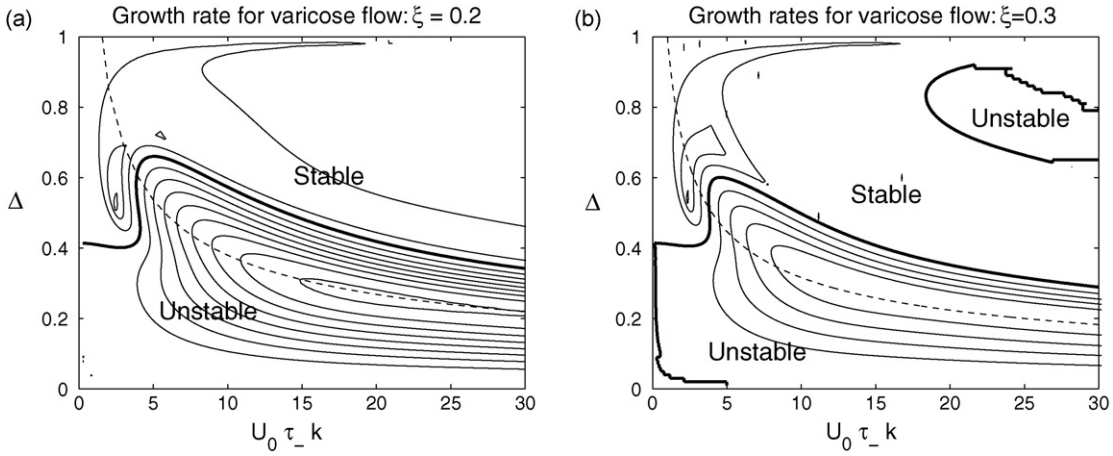

Fig. 16. Coextruded UCM liquids at high *Wi*. Contour plots of growth rate for varicose modes for symmetric Poiseuille flow. The bold line is the marginal stability curve. For $\xi > \xi_c$ there is instability at large $U_0\tau_- k$ holding Δ fixed, while stability exists if $\xi < \xi_c$. The dashed lines show constant $\Delta(U_0\tau_- k)^{1/2}$. (a) Short-waves stable for $\xi = 0.2$ if $\Delta \gg 1/(U_0\tau_- k)^{1/2}$. (b) Short-waves unstable for $\xi = 0.3$ if $\Delta \gg 1/(U_0\tau_- k)^{1/2}$.

constant throughout the interfacial boundary layer. That is, we expect similar behavior as long as $U'/U'' \ll 1/kU'\tau$ at the interface. When these terms are comparable, $U''/kU'^2\tau \sim 1$ and different effects are expected.

When the interfaces are far from the centerline, the linearized equations at the interface are similar to those for Couette flow, and we do indeed find the same stability criteria observed previously. As shown in Fig. 16, if $\xi > \xi_c \approx 0.28$ we find instability at large values of $U_0\tau_- k$ (holding Δ fixed), while there is stability if $\xi < \xi_c$. Some numerical difficulties are evident in Fig. 16(b) where both $U_0\tau_- k$ and Δ are large.

Although the growth rates are the same as for Couette flow, the mode structures are not. We plot the perturbation flow for the Couette-like instability in Figs. 17 and 18. As before, the flow has a boundary layer close to the interface. However, the perturbation decays before reaching the walls, contrasting with the

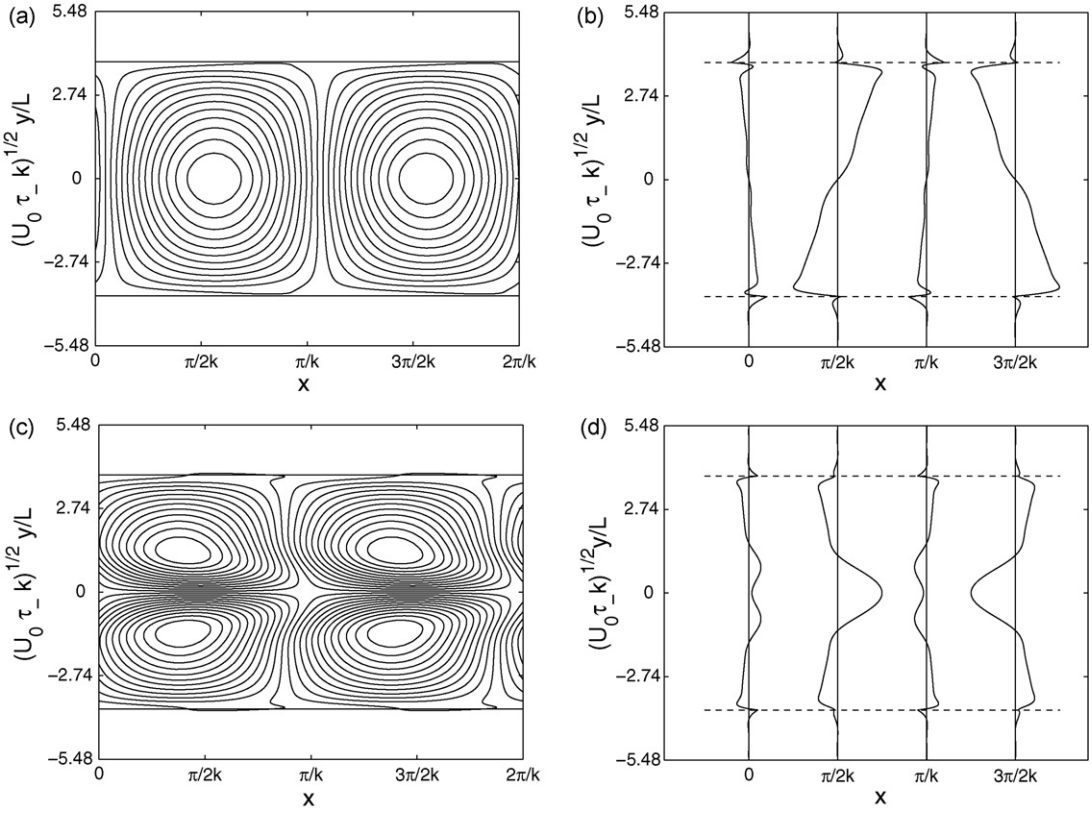

Fig. 17. Coextruded UCM liquids. Perturbation flows for $\xi = 0.5$, $\Delta = 0.7$, and $U_0\tau_- k = 30$. For the varicose mode $\omega\tau_- = 15.6203 + 0.0598i$ and for the sinuous mode $\omega\tau_- = 15.6208 + 0.0590i$. The perturbation flow decays before reaching the walls. (a) Sinuous mode streamlines. (b) Sinuous mode perturbed x-velocity. (c) Varicose mode streamlines. (d) Varicose mode perturbed x-velocity.

Please cite this article in press as: J.C. Miller, J.M. Rallison, Interfacial instability between sheared elastic liquids in a channel, J. Non-Newtonian Fluid Mech. (2007), doi:10.1016/j.jnnfm.2007.01.009

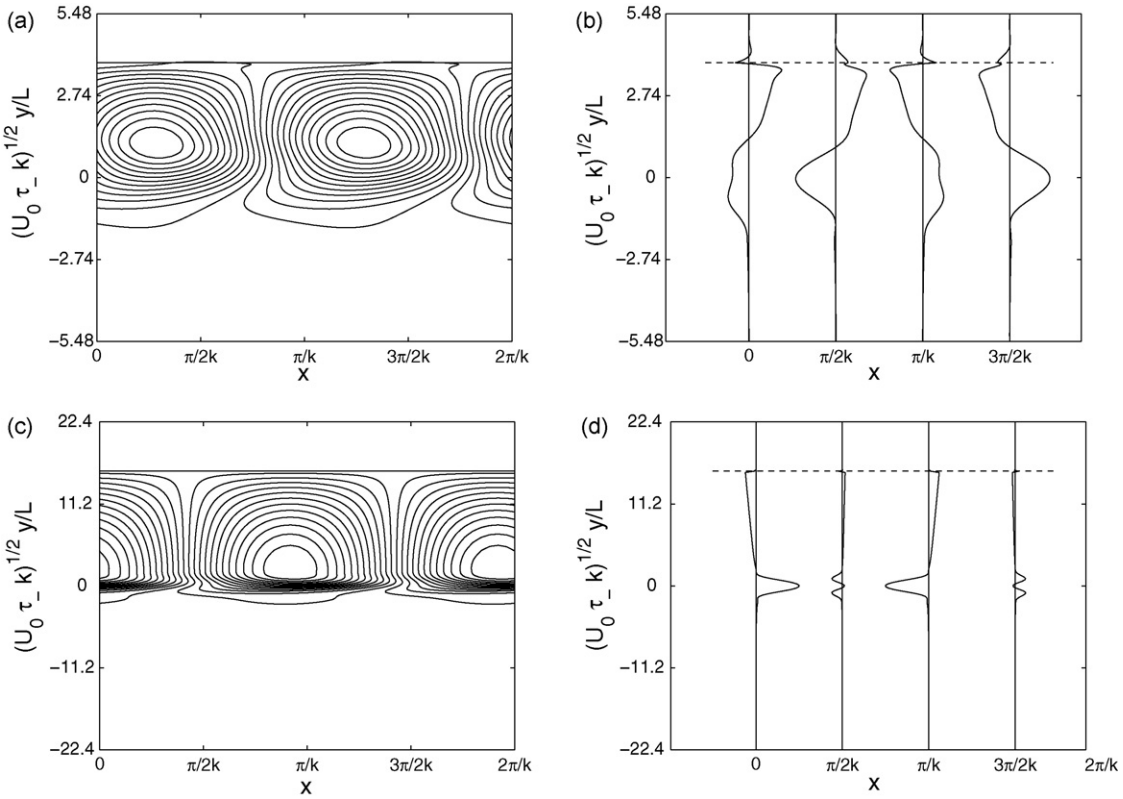

Fig. 18. Coextruded UCM liquids. Perturbation flows with a single interface for $\xi = 0.5$, $\Delta = 0.7$ with $U_0\tau_- k = 30$, 500. For $U_0\tau_- k = 30$, we have $\omega\tau_- = 15.6205 + 0.0594i$ and for $U_0\tau_- k = 500$, $\omega\tau_- = 255.3063 + .0657i$. In both cases the perturbation flow decays before reaching the wall. (a) Streamlines with $U_0\tau_- k = 30$. (b) Perturbed x-velocity with $U_0\tau_- k = 30$. (c) Streamlines with $U_0\tau_- k = 500$. (d) Perturbed x-velocity with $U_0\tau_- k = 500$.

Couette flow case. Between the interface and a boundary layer at the centerline, the flow is similar in appearance to the Couette case, but close to the centerline different effects occur. This region permits a return flow providing zero net mass flux without requiring a significant perturbation in the outer flow. When $\xi = 0.5$ and $U_0\tau_- k = 30$, the values of $\omega\tau_-$ in the frame of reference of the interface are all about $0.32 + 0.06i$ and the value for $U_0\tau_- k = 500$ is about $0.306 + 0.066i$. These are consistent with the result for Couette flow, $\omega\tau_- \to 0.30544 + 0.06603i$ as $U_0\tau_- k \to \infty$ (cf., Fig. 4 where the shear rate has opposite sign).

Fig. 16 suggests that if Δ is comparable with $1/(U_0\tau_- k)^{1/2}$, different behavior arises. This corresponds to the distinguished limit where U'/U'' has the same magnitude as $1/kU'\tau$, discussed in a companion paper [21].

9. Discussion

This paper has considered purely-elastic interfacial instabilities of parallel shear flows of viscoelastic liquids. Previous work on this topic has classified modes on the basis of (dimensional) wavelength and channel width into *long-waves* $k^{-1} \gg L$ and *short-waves* $k^{-1} \ll L$, ignoring the elastic length scale $U_0\tau$. The hidden assumption was made in previous analyses that $k^{-1} \gg U_0\tau$ or $k^{-1} \ll U_0\tau$ respectively. However, the analysis here shows that a different classification should be used: long-waves for which $k^{-1} \gg U_0\tau, L$; wide-channel for which $L \gg k^{-1}, U_0\tau$; and fast-flow for which $U_0\tau \gg L, k^{-1}$. Under this new classification, the distinct behaviors of short-waves at large and small *Wi* are each a special case of a more general class which persists even when the wavelength is long compared to the channel width.

Because there are three length scales, it is perhaps unsurprising that the stability of waves with $kL \ll 1$ and of waves with $kL \gg 1$ cannot offer any guarantee of stability for intermediate k (contrary to the assertion in [22,23]). This is evident in Fig. 16(a) for a range of Δ around 0.5, and is discussed further in a companion paper [21].

There are two surprising features of the fast-flow instability: the first is that the growth rate is determined entirely within a boundary layer at the interface, even though the perturbation flow can fill the entire channel. The second is that the instability persists even with asymptotically large surface tension.

We are not aware of any experiments that have observed the high *Wi* instability predicted in this paper. Nevertheless, the numerical estimates suggest that experimental parameters need not be extreme. For sufficiently viscous Boger liquids with a relaxation time measured in seconds and $\beta > 0.2$, we predict that an instability should be observed for a shear rate of $1\,s^{-1}$, so long as the liquids do not mix. Visualizing the instability may be difficult if surface tension is strong such that the interface is not significantly perturbed.

Please cite this article in press as: J.C. Miller, J.M. Rallison, Interfacial instability between sheared elastic liquids in a channel, J. Non-Newtonian Fluid Mech. (2007), doi:10.1016/j.jnnfm.2007.01.009

Throughout we have assumed that the Reynolds number is zero. This assumption is not required to observe the fast-flow instabilities so long as the flow is laminar. The local Reynolds number based on the shear rate and the thickness of the boundary layer will be small even if the global Reynolds number based on the shear rate and the channel width is large. Consequently inertia is unimportant in the boundary layer and so the instability is expected to persist in the presence of modest inertia.

We have assumed that the interface is sharp. In general the width of the interface will be on the molecular scale, much smaller than any length scale considered in this paper. Under the continuum hypothesis, it is safe to assume zero width. If the liquids have very weak surface tension however, they may diffuse into one another, yielding a mixed layer. If the length scale of this mixed layer becomes comparable to the length scale of the boundary layer governing stability, then our results must change. Earlier work at moderate *Wi* has shown that this blurring leads to stability [13].

Instability occurs for infinite surface tension because the normal force balance at the interface decouples from the rest of the analysis and plays no role. This observation conflicts with a widely-held assumption about the driving force for purely elastic interfacial instabilities namely [24]:

> *the mechanism of purely elastic interfacial instabilities has been demonstrated to be the coupling of the jump in base flow normal stresses across the interface and the perturbation velocity field.*

This statement may be true for many purely elastic interfacial instabilities and is certainly the case for long-wave instabilities. However, since the jump in base flow normal stress disappears from the analysis in the limiting case, a distinct mechanism must be involved. Our results provide some restrictions on the stability mechanism. The stability does not depend on the details of the flow except within a thin layer about the interface. It does not depend on a perturbation to the interface and can occur with infinite surface tension. Because the mode travels relative to the interface at leading order, the mechanism must depend on the sign of the shear rate. We have not been able to isolate the mechanism.

Acknowledgments

Some of this work was done while JCM visited the Institute of Theoretical Geophysics, University of Cambridge. JCM was supported under a National Science Foundation Graduate Research Fellowship and by the Department of Energy at LANL under Contract No. DE-AC52-06NA25396 and the DOE Office of ASCR program in Applied Mathematical Sciences.

Appendix A. Linear perturbation equations

We consider the stability of the flow to infinitesimal disturbances. These disturbances change the velocity field $\boldsymbol{U}$, the stress Σ, and in general the interface location Δ. We use lower case letters $\boldsymbol{u}$, σ, and δ to denote the corresponding perturbations.

The perturbation quantities are small and may be taken to be proportional to $\exp(ikx - i\omega t)$. We take $\boldsymbol{u} = (\mathrm{D}\psi, -ik\psi)$ to satisfy incompressibility automatically. 'D' denotes differentiation with respect to y.

The perturbed stress σ satisfies

$$\sigma = -p\mathsf{I} + \mu\left(2\beta\mathsf{e} + \frac{1-\beta}{\tau}\mathsf{A}\right),$$

where the perturbation rate of strain is

$$\mathsf{e} = \begin{pmatrix} ik\mathrm{D}\psi & (\mathrm{D}^2+k^2)\psi/2 \\ (\mathrm{D}^2+k^2)\psi/2 & -ik\mathrm{D}\psi \end{pmatrix}.$$

The momentum equation $\nabla\cdot\Sigma = \mathbf{0}$ gives

$$ik\sigma_{11} + \mathrm{D}\sigma_{12} = 0, \tag{A.1}$$

$$ik\sigma_{12} + \mathrm{D}\sigma_{22} = 0. \tag{A.2}$$

Taking the curl of the momentum equation and substituting for σ we find the vorticity equation

$$\beta(\mathrm{D}^2-k^2)^2\psi + \frac{1-\beta}{\tau}[ik\mathrm{D}(a_{11}-a_{22}) + (\mathrm{D}^2+k^2)a_{12}] = 0. \tag{A.3}$$

The evolution equations for a are

$$\alpha a_{11} = 2\frac{U_0}{L}a_{12} + 2ik\left(2\frac{U_0^2\tau^2}{L^2}+1\right)\mathrm{D}\psi + 2\frac{U_0\tau}{L}\mathrm{D}^2\psi, \tag{A.4}$$

$$\alpha a_{12} = \frac{U_0}{L}a_{22} + k^2\left(2\frac{U_0^2\tau^2}{L^2}+1\right)\psi + \mathrm{D}^2\psi, \tag{A.5}$$

$$\alpha a_{22} = 2k^2\frac{U_0\tau}{L}\psi - 2ik\mathrm{D}\psi, \tag{A.6}$$

where $\alpha = -i\omega + ikU_0y/L + 1/\tau$.

The no-slip boundary conditions at the wall are

$$\psi = \mathrm{D}\psi = 0 \quad \text{at} \quad y = (1-\Delta)L, -\Delta L. \tag{A.7}$$

Continuity of velocity at the interface $y = 0$ gives

$$[\![\psi]\!] = [\![\mathrm{D}\psi]\!] = 0. \tag{A.8}$$

The perturbed interface lies at $y = \delta$, and the interface normal becomes $\boldsymbol{N}+\boldsymbol{n}$ where $\boldsymbol{n} = (-ik\delta, 0)$. To linear order the interfacial condition $[\![\Sigma+\Sigma]\!]\cdot(\boldsymbol{N}+\boldsymbol{n}) = \gamma\kappa(\boldsymbol{N}+\boldsymbol{n})$ becomes

$$-2ik(1-\beta)[\![\tau]\!]U_0^2\delta/L^2 + \beta[\![\mathrm{D}^2\psi]\!] + (1-\beta)\left[\!\left[\frac{a_{12}}{\tau}\right]\!\right] = 0, \tag{A.9}$$

$$\left[\!\left[-\frac{\beta}{ik}\mathrm{D}^3\psi + \frac{(1-\beta)}{\tau}\left(-\frac{\mathrm{D}a_{12}}{ik} + a_{22} - a_{11}\right)\right]\!\right] = \frac{\gamma k^2}{\mu}\delta, \tag{A.10}$$

where we have used Eq. (A.1) to eliminate the pressure from (A.10). These equations correspond to Eqs. (15) and (16) of [11] with the addition of surface tension.

Please cite this article in press as: J.C. Miller, J.M. Rallison, Interfacial instability between sheared elastic liquids in a channel, J. Non-Newtonian Fluid Mech. (2007), doi:10.1016/j.jnnfm.2007.01.009

The interface is a material surface and so $(\partial_t + [\boldsymbol{U} + \boldsymbol{u}] \cdot \nabla)\delta = -ik\psi$. Thus since the base state velocity vanishes at the interface

$$\delta = \frac{k\psi}{\omega}, \tag{A.11}$$

where ψ is evaluated at $y = 0$.

The Eqs. (A.3)–(A.11) define the eigenvalue problem for the complex growth rate ω.

Appendix B. Analytic solutions

For the UCM liquid ($\beta = 0$) Gorodtsov and Leonov [25] explicitly found the streamfunction ψ solving (9)–(12) by substituting for the a_{ij} in (9) and factoring the resulting differential operator. We generalize their factorization and use this to give the solution for arbitrary β. We record the solution and limiting cases below for future reference.

Combining the constitutive Eqs. (10)–(12) with the vorticity Eq. (9) we find

$$\left(\alpha^2 \mathrm{D}^2 - 2i\alpha\mathrm{D} - 2 - \frac{\alpha^2}{Wi^2}\right) \times \left([s\tau\alpha + 1]\mathrm{D}^2 + 2i\tau\mathrm{D} - 2\tau^2 - \frac{s\tau\alpha + 1}{Wi^2}\right)\psi = 0,$$

where $s = \beta/(1-\beta)$. This gives the explicit solution

$$\begin{aligned}\psi(y) = {} & C_1(y-\omega)\exp\left(\frac{y}{Wi}\right) + C_2(y-\omega)\exp\left(-\frac{y}{Wi}\right) \\ & + C_3\exp\left(\frac{y}{Wi}\right)\ \mathcal{M}\left(\frac{1}{s}(1+i\tau Wi), \frac{2}{s}, \frac{2i}{Wi}\left(\alpha+\frac{1}{s\tau}\right)\right) \\ & + C_4\exp\left(\frac{y}{Wi}\right)\ \mathcal{U}\left(\frac{1}{s}(1+i\tau Wi), \frac{2}{s}, \frac{2i}{Wi}\left(\alpha+\frac{1}{s\tau}\right)\right),\end{aligned} \tag{B.1}$$

where $\mathcal{M}$ and $\mathcal{U}$ are Kummer's functions [26]. This solution is equivalent to one found by Wilson et al. [15]. In practice we do not find this solution to be useful for our stability problem and so we turn instead to numerics to solve the Eqs. (9)–(18) when β is nonzero.

In the $\beta = 0$ limit, the solution found by Gorodtsov and Leonov [25]

$$\begin{aligned}\psi(y) = {} & C_1(y-\omega)\exp\left(\frac{y}{Wi}\right) + C_2(y-\omega)\exp\left(-\frac{y}{Wi}\right) \\ & + C_3\exp\left[\tau y\left(-i - \sqrt{1 + \frac{1}{\tau^2 Wi^2}}\right)\right] \\ & + C_4\exp\left[\tau y\left(-i + \sqrt{1 + \frac{1}{\tau^2 Wi^2}}\right)\right]\end{aligned} \tag{B.2}$$

is more amenable to asymptotic analysis. From this solution we see that if Wi is large (but less than the dimensionless channel width k) there are two boundary layers, one with thickness of order unity and another with thickness of order Wi.

The solution at large Wi for the Oldroyd-B liquid is

$$\begin{aligned}\psi(y) = {} & C_1(y-\omega) + C_2 y(y-\omega) + C_3\left(\alpha + \frac{1}{s\tau}\right)^{(s-2/2s)} \\ & \times \mathcal{J}_{(s-2/s)}\left(2i\sqrt{2}\frac{(-1-\alpha)^{1/2}}{s}\right) \\ & + C_4\left(\alpha + \frac{1}{s\tau}\right)^{(s-2/2s)} \mathcal{Y}_{(s-2/s)}\left(2i\sqrt{2}\frac{(-1-\alpha)^{1/2}}{s}\right),\end{aligned} \tag{B.3}$$

where $\mathcal{J}$ and $\mathcal{Y}$ are Bessel functions [26]. For a UCM liquid ($\beta = 0$) at large Wi we find

$$\psi(y) = C_1(y-\omega) + C_2 y(y-\omega) + C_3 e^{(-1-i)\tau y} + C_4 e^{(1-i)\tau y}. \tag{B.4}$$

The $\exp(\pm y/Wi)$ terms in Eq. (B.2) have been replaced by algebraic terms. This reflects the fact that the thickness of the corresponding boundary layer has become large compared to the channel width.

Appendix C. Numerical methods

In principle we can find ψ analytically, but if k is finite or if $\beta \neq 0$, it is more convenient in practice to solve the problem numerically. We use two methods which provide results consistent with one another as well as with the analytic limits presented and which reproduce previous results.

The first method is orthogonal shooting [27,10,11]. At each wall we have two free conditions. Using an initial guess for ω we integrate two independent solutions from the bottom wall to the top. The boundary conditions at the top wall define a 2×2 matrix whose determinant is zero when ω is an eigenvalue. We refine our guess for ω by Newton–Raphson iteration and use parameter continuation to follow the modes through parameter space. Previous studies have used an orthogonalization during the integration, but we have not found this to be necessary. Our implementation reproduces earlier results from [10–12,15]. Some numerical difficulties were encountered for large or small values of k as detailed below. Parameter continuation sometimes finds another mode if the step in parameter is too large.

The second method is a spectral algorithm as in [28,29,15]. We expand the ψ and a_{ij} variables as sums of Chebyshev polynomials. The linear problem reduces to the form $\mathsf{A}\ \boldsymbol{v} = i\omega\mathsf{B}\ \boldsymbol{v}$ where A and B are square matrices and $\boldsymbol{v}$ is a vector containing the coefficients of the expansions for ψ and a_{ij}. The method works best if all equations and variables are kept to a self-consistent accuracy. We keep the vorticity Eq. (9) to N terms, Eq. (10) to $N+1$ terms and Eqs. (11) and (12) to $N+2$ terms. We keep ψ, a_{11}, a_{12}, and a_{22} to $N+4$, $N+1$, $N+2$, and $N+2$ terms respectively. The eigenvalues are found through Matlab's `eig` and `eigs` algorithms. Again we are able to repeat earlier calculations.

Please cite this article in press as: J.C. Miller, J.M. Rallison, Interfacial instability between sheared elastic liquids in a channel, J. Non-Newtonian Fluid Mech. (2007), doi:10.1016/j.jnnfm.2007.01.009

The spectral method does not need a good initial guess to find each eigenvalue. Further, it behaves better for large k. However, it is computationally slower. In addition there is a continuous spectrum of modes where $\alpha = 0$, and the spectral method requires many polynomials to resolve modes with ω close to this line [15].

We use the spectral algorithm to find modes and then parameter continuation with either algorithm to follow them. Modes disappear into (or emerge out of) the continuous spectrum [15], so we cannot guarantee that all modes have been found though we do find all modes predicted in the $k \to 0$ or $k \to \infty$ limits. If any modes have been missed, they exist only at intermediate wavenumbers.

References

[1] Y. Renardy, Stability of the interface in two-layer Couette flow of upper convected Maxwell liquids, J. Non-Newtonian Fluid Mech. 28 (1988) 99–115.
[2] R.G. Larson, Instabilities in viscoelastic flows, Rheol. Acta 31 (1992) 213–263.
[3] E.S.G. Shaqfeh, Purely elastic instabilities in viscometric flows, Annu. Rev. Fluid Mech. 28 (1996) 129–185.
[4] K.-P. Chen, Interfacial instability due to elastic stratification in concentric coextrusion of two viscoelastic fluids, J. Non-Newton. Fluid Mech. 40 (1991) 155–175.
[5] K.-P. Chen, D.D. Joseph, Elastic short wave instability in extrusion flows of viscoelastic liquids, J. Non-Newton. Fluid Mech. 42 (1992) 189–211.
[6] E.J. Hinch, O.J. Harris, J.M. Rallison, The instability mechanism for two elastic liquids being co-extruded, J. Non-Newton. Fluid Mech. 43 (1992) 311–324.
[7] H.K. Ganpule, B. Khomami, A theoretical investigation of interfacial instabilities in the three layer superposed channel flow of viscoelastic fluids, J. Non-Newton. Fluid Mech. 79 (1998) 315–360.
[8] H.K. Ganpule, B. Khomami, The effect of transient viscoelastic properties on interfacial instabilities in superposed pressure driven channel flows, J. Non-Newton. Fluid Mech. 80 (1999) 217–249.
[9] H.K. Ganpule, B. Khomami, An investigation of interfacial instabilities in the superposed channel flow of viscoelastic fluids, J. Non-Newton. Fluid Mech. 81 (1999) 27–69.
[10] H.J. Wilson, Shear flow instabilities in viscoelastic fluids, Ph.D. thesis, Cambridge University, Cambridge, United Kingdom, 1998.
[11] H.J. Wilson, J.M. Rallison, Short wave instability of co-extruded elastic liquids with matched viscosities, J. Non-Newton. Fluid Mech. 72 (1997) 237–251.
[12] H.J. Wilson, J.M. Rallison, Instability of channel flow of a shear-thinning White–Metzner fluid, J. Non-Newton. Fluid Mech. 87 (1999) 75–96.
[13] H.J. Wilson, J.M. Rallison, Instability of channel flows of elastic liquids having continuously stratified properties, J. Non-Newton. Fluid Mech. 85 (1999) 273–298.
[14] M. Renardy, On the stability of parallel shear flow of an Oldroyd-B fluid, Diff. Integr. Eqs. 6 (3) (1993) 481–489.
[15] H.J. Wilson, M. Renardy, Y. Renardy, Structure of the spectrum in zero Reynolds number shear flow of the UCM and Oldroyd-B liquids, J. Non-Newton. Fluid Mech. 80 (1999) 251–268.
[16] R. Ghisellini, Elastic free energy of an upper-convected Maxwell fluid undergoing a fully developed planar Poiseuille flow: a variational result, J. Non-Newton. Fluid Mech. 46 (1993) 229–241.
[17] R. Kupferman, On the linear stability of plane Couette flow for an Oldroyd-B fluid and its numerical approximation, J. Non-Newton. Fluid Mech. 127 (2005) 169–190.
[18] C.R. Doering, B. Eckhardt, J. Schumacher, Failure of energy stability in Oldroyd-B fluids at arbitrarily low Reynolds numbers, J. Non-Newton. Fluid Mech. 135 (2006) 92–96.
[19] K. Atalik, R. Keunings, Non-linear temporal stability analysis of viscoelastic plane channel flows using a fully-spectral method, J. Non-Newton. Fluid Mech. 102 (2002) 299–319.
[20] C.-T. Huang, B. Khomami, The instability mechanism of single and multilayer Newtonian and viscoelastic flows down an inclined plane, Rheol. Acta 40 (5) (2001) 467–484.
[21] J.C. Miller, J.M. Rallison, Instability of coextruded elastic liquids at high Weissenberg number, submitted for publication.
[22] P. Laure, H.L. Meur, Y. Demay, J.C. Saut, S. Scotto, Linear stability of multilayer plane Poiseuille flows of Oldroyd-B fluids, J. Non-Newton. Fluid Mech. 71 (1997) 1–23.
[23] S. Scotto, P. Laure, Linear stability of three-layer Poiseuille flow for Oldroyd-B fluids, J. Non-Newton. Fluid Mech. 83 (1999) 71–92.
[24] B. Lin, B. Khomami, R. Sureshkumar, Effect of non-normal interactions on the interfacial instability of multilayer viscoelastic channel flows, J. Non-Newton. Fluid Mech. 116 (2004) 407–429.
[25] V.A. Gorodtsov, A.I. Leonov, On a linear instability of a plane parallel Couette flow of viscoelastic fluid, J. Appl. Math. Mech. 31 (2) (1967) 310–319.
[26] M. Abramowitz, I.A. Stegun, Handbook of Mathematical Functions with Formulas, Graphs, and Mathematical Tables, Dover Publications, Inc., New York, 1965.
[27] T.C. Ho, M.M. Denn, Stability of plane Poiseuille flow of a highly elastic liquid, J. Non-Newton. Fluid Mech. 3 (1977) 179–195.
[28] J.P. Boyd, Chebyshev, Fourier Spectral Methods, second ed., Dover Publications, Inc., New York, 2001.
[29] J.J. Dongarra, B. Straughan, D.W. Walker, Chebyshev tau-QZ algorithm methods for calculating spectra of hydrodynamic stability problems, Appl. Numeric. Math.: Trans. IMACS 22 (4) (1996) 399–434.

Please cite this article in press as: J.C. Miller, J.M. Rallison, Interfacial instability between sheared elastic liquids in a channel, J. Non-Newtonian Fluid Mech. (2007), doi:10.1016/j.jnnfm.2007.01.009